

# Group Distributionally Robust Optimization can Suppress Class Imbalance Effect in Network Traffic Classification

Wumei Du <sup>\*1</sup> Qi Wang <sup>\*1</sup> Yiqin Lv <sup>1</sup> Dong Liang <sup>#1</sup> Guanlin Wu <sup>2</sup> Xingxing Liang <sup>2</sup> Zheng Xie <sup>#1</sup>

## Abstract

Internet services have led to the eruption of traffic, and machine learning on these Internet data has become an indispensable tool, especially when the application is risk-sensitive. This paper focuses on network traffic classification in the presence of class imbalance, which fundamentally and ubiquitously exists in Internet data analysis. This existence of class imbalance mostly drifts the optimal decision boundary, resulting in a less optimal solution for machine learning models. To alleviate the effect, we propose to design strategies for alleviating the class imbalance through the lens of group distributionally robust optimization. Our approach iteratively updates the non-parametric weights for separate classes and optimizes the learning model by minimizing reweighted losses. We interpret the optimization steps from a Stackelberg game and perform extensive experiments on typical benchmarks. Results show that our approach can not only suppress the negative effect of class imbalance but also improve the comprehensive performance in prediction.

## 1. Introduction

The past few decades have witnessed a surge in Internet traffic due to the quick development of the Internet of Things (IoTs) (Rose et al., 2015) and the great demand for data resources for training machine learning models. The potential value of increasing Internet traffic also brings many concerns, and security is the most crucial factor in Internet services. To prevent hacker attacks, malware, phishing, etc., and protect users' privacy, the technical staff encapsulates most network traffic according to encryption protocols before it is transmitted.

<sup>\*</sup>Equal contribution <sup>1</sup>College of Science, National University of Defense Technology, Changsha, China <sup>2</sup>College of Defense, Peking, China. Correspondence to: Dong Liang and Zheng Xie <[dongliangnudt@nudt.edu.cn](mailto:dongliangnudt@nudt.edu.cn); [xiezheng81@nudt.edu.cn](mailto:xiezheng81@nudt.edu.cn)>.

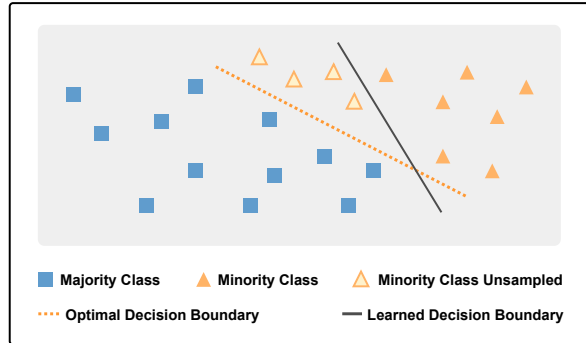


**Figure 1. Drift of decision boundary in binary classification.** Due to the nature of the class imbalance, the machine learning obtained decision boundary tends to deviate from the optimal one.

Considering the inherent risk sensitivity to applications, there has been growing increasingly interest in analyzing these encrypted traffic data with the help of machine learning methods. Particularly, traffic classification has played an essential role in network security, privacy protection, network management, and threat detection (Nguyen & Armitage, 2008). Through in-depth research and development of relevant technologies and methods, we can effectively deal with the challenges brought by encrypted traffic and enhance network security.

**Existing Challenges:** When it comes to traffic data classification, there emerge several challenges. Unlike general class imbalance learning problems, the classes of traffic data are mostly numerous, and there is a high imbalance among classes. Particularly, as illustrated in Figure 2, the small but crucial classes, such as malicious traffic, tend to occupy a small proportion of the whole dataset. These traits in statistics cause the prevalent machine learning models to suffer a crucial issue, which is termed the *decision boundary shift* in the literature (Wang et al., 2017; Douzas & Bacao, 2018; Das et al., 2022; Huang et al., 2023). As illustrated in Figure 1, examples of the minority class near the oracle boundary can be easily identified as the majority class by the classifier due to the boundary shift. To alleviate such an effect, researchers have developed a collection of strategies, such as data augmentation, under/over-sampling, cost-sensitive learning, and so forth. *Even so, obtaining a robust classification model in a simple yet effective way is*

still challenging. Among existing techniques, data augmentation methods and cost-sensitive learning methods enjoy special popularity. The family of data augmentation relies on sampling strategies, generative models, or other mix-up tricks (Elreedy & Atiya, 2019; Chou et al., 2020; Zhao et al., 2021). Such a family either requires a particular configuration in sampling ratios (Liu et al., 2008; Shelke et al., 2017) or can easily produce unnatural instances (Sampath et al., 2021). Benefiting from diverse available mechanisms, the cost-sensitive family is more flexible in configurations (Madabushi et al., 2019; Fernando & Tsokos, 2021), nevertheless, these mechanisms are mostly heuristic and not versatile in practice.

**Research Motivations & Methods:** Largely inspired by group distributionally robust optimization (Sagawa et al., 2019; Rahimian & Mehrotra, 2022), we establish connections between distributional robustness and cost-sensitive strategies and present a novel approach to resolving the traffic class imbalance issue. In circumventing the complicated mechanism design, we propose to *employ the adaptive risk minimization principle and interpret the optimization process from the Stackelberg game*. In detail, we cluster classes into different groups and dynamically assign weights to their loss functions at a group level. The critical insight is that classification results over the minority classes can be viewed as the worst cases in optimization, and we can take the intermediate results into optimization. Such a design is *agnostic to the traffic dataset and can stably schedule the group cost weights* for class performance balance.

**Primary Contributions & Outlines:** The remainder is organized as follows. Section 2 summarizes the literature work on traffic data classification. In Section 3, we introduce mathematical notations and necessary preliminaries. Then, we present the developed approach in Section 4. The experimental results and analysis are reported in Section 5, followed by the conclusion and future extension. To sum up, our contribution is two-fold:

1. Through the lens of group distributionally robust optimization, we present a simple yet effective cost-sensitive approach to address the class imbalance issue by scheduling the weights of grouped classes.
2. The optimization steps in our approach can be interpreted as approximately resolving a Stackelberg game, and we constitute the concept of equilibrium as the robust solution in traffic class imbalance learning.

We conduct extensive experiments to examine the performance of the proposed method on a collection of commonly used benchmarks. The empirical results show that our approach does not require complicated hyper-parameter configurations and can achieve superior performance over existing typical baselines in network traffic classification.

## 2. Literature Review

**Background Knowledge of Encrypted Traffic.** Specifically, the sender converts the plaintext data packet into ciphertext through an encryption algorithm and then packages the ciphertext into an encrypted data packet for transmission according to the encryption protocol. Only when the receiver has the corresponding decryption algorithm can the encrypted data packet be decrypted and processed, thereby effectively protecting the data packet's confidentiality, integrity, and security and preventing it from being detected, attacked, and tampered with during network transmission. As the computing capabilities of computers, mobile terminals, and other devices continue to improve, various encryption technologies and encryption protocols are constantly updated, resulting in the rapid growth of encrypted traffic data. At the same time, encryption technology provides opportunities for many unscrupulous cyber criminals. Various types of malware and cyber attacks also use encryption to avoid detection by various network defense security systems. Network traffic classification is generally the prerequisite for network intrusion detection and an essential task in network security.

**Categories on Traffic Class Imbalanced Learning Methods.** To alleviate the effect of class imbalance, researchers have developed a collection of strategies, which can be mainly divided into three categories:

(i) Under/Over-sampling aims to reduce the size of the majority classes and increase that of the minority classes respectively in the learning process, forcing almost equal quantities relative to each other (Xie et al., 2020; Park & Park, 2021; Zuech et al., 2021). Random Under Sampling (RUS) and Random over sampling (ROS) are two classical approaches. RUS randomly removes some majority classes' samples which might lead to information loss (Lotfollahi et al., 2020), while ROS produces copies for minority classes to achieve balance. Synthetic Minority Over-sampling Technique (SMOTE) (Chawla et al., 2002; Yan et al., 2018; Zhang et al., 2020) creates synthetic samples rather than copies, which is proven to be effective in imbalanced network traffic classification, but it tends to introduce noise and causes instability in learning (Guo et al., 2021).

(ii) Data augmentation focuses on density estimation and sample generative mechanism. By leveraging existing dataset, the generative artificial intelligence models (Wang et al., 2023) can sample more synthetic samples for the minority class (Zavruk & Iskefiyeli, 2020; Guo et al., 2021; Lin et al., 2022; Monshizadeh et al., 2021; Khanam et al., 2022; D'Angelo & Palmieri, 2021; Bårli et al., 2021; Xu et al., 2020). Several studies report impressive performance based on deep generative models for data augmentation, especially the Generative Adversarial Network (GAN) (Goodfellow et al., 2014). Despite the potential of GAN-based data aug-

mentation methods (Guo et al., 2021; Wang et al., 2020; Ding et al., 2022), the generative process sometimes produces samples from the low-density region and results in unsatisfactory minority ones. Meanwhile, generative models are challenging in stable training and suffer from mode collapse, which sometimes leads to the lack of diversity of generated samples.

(iii) The mechanism of cost-sensitive learning is to reweight the costs of various classes in the training process. The role of class-specific weights is to penalize the case when the classification of the minority is severely under performance in the optimization process. Some researchers integrated the class-specific costs with the loss function for deep learning classification on imbalanced datasets (Wang et al., 2016; Khan et al., 2017; Gupta et al., 2022; Telikani & Gandomi, 2021). The earlier work that introduced cost-sensitive learning to handle class imbalance problem in network security is in intrusion detection for IoTs (Telikani & Gandomi, 2021). Subsequently, some deep learning frameworks that adopt this strategy have been developed for network traffic classification on unbalanced traffic data, such as stacked autoencoder and convolution neural networks (Telikani et al., 2021), support vector machine (Dong, 2021), and recurrent neural networks (Zhu et al., 2023b). Most of these cases are heuristic in class weight assignment. In view of the flexibility in configurations of the cost-sensitive learning, we try to trade off the overall performance and computational efficiency by dynamically assigning cost weights at a group level.

### 3. Preliminaries

**Notations.** Let  $\mathbf{x} \in \mathcal{X} \subseteq \mathbb{R}^d$  be the vector of each traffic data as the input for classification. We denote the prediction label for each input feature by  $y \in \mathcal{Y} = \{1, 2, \dots, \mathcal{C}\}$ . The classification model is expressed as  $\boldsymbol{\theta} \in \Theta$ . We write the distribution of data points as  $p(\mathbf{x}, y)$ . The dataset of interest is  $D = \{(\mathbf{x}_i, y_i)\}_{i=1}^N$ , where  $N$  is the number of training samples. We partition the dataset into  $D = \bigcup_{c=1}^{\mathcal{C}} D_c$ , where  $D_c$  denotes the data points that belong to the class  $c$ .

The goal in network traffic classification is to learn a map  $f_{\boldsymbol{\theta}} : \mathcal{X} \mapsto \mathcal{Y}$  that tries to minimize the classification errors, e.g.,  $\mathbb{E}_{p(\mathbf{x}, y)} [\mathbb{1}[f_{\boldsymbol{\theta}}(\mathbf{x}) \neq y]]$ , as much as possible. The following will detail the classification model and fundamental knowledge about the Stackelberg game, which are prerequisites for our developed method.

#### 3.1. Multiclass Imbalanced Learning

We employ deep learning models for multiclass imbalanced network traffic classification. The fully connected deep neural networks (DNNs) are constructed as the backbone for generality to enable multiclass classification. In mathemat-

ics, the DNN consists of the feature extraction module  $\Phi = \{\mathbf{W}^i, \mathbf{b}^i\}_{i=1}^H$  and the output module  $\Phi_o = \{\mathbf{W}_c^o, b_c^o\}_{c=1}^{\mathcal{C}}$ . Hence, the estimated probability of a data point  $(\mathbf{x}, y)$  for all classes can be computed as:

$$p(\hat{y} = c | \mathbf{x}; \boldsymbol{\theta}) = \frac{\exp(\Phi(\mathbf{x})^T \mathbf{W}_c^o + b_c^o)}{\sum_{i=1}^{\mathcal{C}} \exp(\Phi(\mathbf{x})^T \mathbf{W}_i^o + b_i^o)}, \quad (1)$$

where the model parameter is  $\boldsymbol{\theta} := \{\Phi, \Phi_o\}$  and  $\hat{y}$  is the predicted result.

Furthermore, we can introduce  $\mathcal{L}(D; \boldsymbol{\theta})$  the negative log-likelihood (NLL) as the loss function in multiclass classification with the help of Eq. (1):

$$\min_{\boldsymbol{\theta} \in \Theta} \mathcal{L}(D; \boldsymbol{\theta}) := \sum_{i=1}^N \sum_{c=1}^{\mathcal{C}} -\mathbb{1}[y_i = c] \ln p(\hat{y}_i = c | \mathbf{x}_i; \boldsymbol{\theta}). \quad (2)$$

#### 3.2. Stackelberg Game

The two-player Stackelberg game is a strategic interaction model frequently utilized in game theory. In such a game, two competitive players engage in a sequential decision-making process to maximize their utility functions. The leader player  $\mathcal{P}_L$  makes decisions first, followed by the follower player, referred to as  $\mathcal{P}_F$ , who makes decisions subsequently after accessing the leader's decisions. This work focuses on a two-player zero-sum Stackelberg game, which can be mathematically depicted as  $\mathcal{SG} := (\mathcal{P}_L, \mathcal{P}_F; \{\boldsymbol{\eta} \in \Delta_c\}, \{\boldsymbol{\theta} \in \Theta\}; \mathcal{F}(\boldsymbol{\eta}, \boldsymbol{\theta}))$ .  $\Delta_c$  (resp.  $\Theta$ ) represents the action space for player  $\mathcal{P}_L$  (resp. player  $\mathcal{P}_F$ ), and  $\mathcal{F}(\boldsymbol{\eta}, \boldsymbol{\theta})$  (resp.,  $-\mathcal{F}(\boldsymbol{\eta}, \boldsymbol{\theta})$ ) represents player  $\mathcal{P}_L$ 's (resp., player  $\mathcal{P}_F$ 's) utility function.

Central to the Stackelberg game is the concept of strategic leadership, whereby the leader's actions influence the follower's subsequent decisions. Being aware of this influence, the leader strategically chooses its actions to maximize its utility while considering the follower's response. Conversely, recognizing the leader's choices, the follower optimizes its decisions accordingly.

Thus, the equilibrium of  $\mathcal{SG}$  can be solved by *backward induction*, that is,

$$\begin{aligned} \max_{\boldsymbol{\eta} \in \Delta_c} \mathcal{F}(\boldsymbol{\eta}, \boldsymbol{\theta}_*(\boldsymbol{\eta})) \quad & \text{s.t. } \boldsymbol{\theta}_*(\boldsymbol{\eta}) = \arg \min_{\boldsymbol{\theta} \in \Theta} \mathcal{F}(\boldsymbol{\eta}, \boldsymbol{\theta}) \\ & \quad \text{(3.a: Leader's Decision-Making)} \\ \min_{\boldsymbol{\theta} \in \Theta} \mathcal{F}(\boldsymbol{\eta}, \boldsymbol{\theta}). \quad & \quad \text{(3.b: Follower's Decision-Making)} \end{aligned}$$

Note that the constraint in Eq. (3.a) is called the leader player  $\mathcal{P}_L$ 's *best response function* in game theory. Such a sequential structure inherently offers the leader a strategic

advantage, as it can anticipate and preempt the follower’s reactions. Consequently, the Stackelberg game is characterized by an asymmetric power dynamic between the leader and follower, where the leader’s strategic precommitment shapes the subsequent interaction between the players.

## 4. Group Distributionally Robust Class Imbalance Learner

As previously mentioned, the existence of class imbalance tends to result in decision boundary drift, which can be risky or even lead to catastrophic results in network traffic classification scenarios. One plausible way to alleviate this effect is to penalize the classification errors via adjusting weights to individual classes (Zhang et al., 2017; Chou et al., 2020). Nevertheless, effectively enabling weight assignment in training processes remains a tricky problem, and there is a limited mechanism for explaining the process. To this end, we introduce **Group Distributionally Robust Class Imbalance Learner (GDR-CIL)** as a competitive candidate method in this section to address the issue. Please refer to Algorithm 1 for details.

### 4.1. Distributional Robustness

This work reduces the decision boundary shift in class imbalance learning to the distributional robustness issue (Sagawa et al., 2019; Rahimian & Mehrotra, 2022). Here, we consider the robustness regarding the classification performance of the minority classes.

To this end, we can translate the optimization problem in the presence of class imbalance as follows:

$$\max_{\boldsymbol{\eta} \in \Delta_c} \min_{\boldsymbol{\theta} \in \Theta} \mathcal{F}(\boldsymbol{\eta}, \boldsymbol{\theta}) := \mathbb{E}_{p(D)} [\boldsymbol{\eta}^\top \mathcal{L}_c(D; \boldsymbol{\theta})] + \lambda \mathcal{R}(\boldsymbol{\eta}), \quad (4)$$

where the loss term  $\mathcal{L}_c(D; \boldsymbol{\theta}) = [\ell(D_1; \boldsymbol{\theta}), \dots, \ell(D_c; \boldsymbol{\theta})]^\top$  denotes the vector of losses for each class. Moreover,  $\boldsymbol{\eta}$  corresponds to an element in  $\Delta_c$  which is the  $(c - 1)$ -dimensional simplex and the term  $\mathcal{R}(\boldsymbol{\eta})$  works as a regularization to avoid the collapse of  $\boldsymbol{\eta}$  into vertices.

The maxmin optimization problem in Eq. (4) can be understood as a two-player zero-sum Stackelberg game (Breton et al., 1988; Li & Sethi, 2017). The leader  $\mathcal{P}_L$  adjusts the weights for different classes over the probability simplex aiming to maximize  $\mathcal{F}(\boldsymbol{\eta}, \boldsymbol{\theta})$ . The minimization operator executes in the parameter space, corresponding to the follower  $\mathcal{P}_F$  in  $\mathcal{SG}$  with the utility function  $-\mathcal{F}(\boldsymbol{\eta}, \boldsymbol{\theta})$ .

### 4.2. Construction of Surrogate Loss Functions

Unlike previous methods, this work reduces class imbalance learning to a distributionally robust optimization at a class group level (Sagawa et al., 2019). We make a hypothesis

that multi-classes retain unobservable group structures in losses, and placing various weights over a collection of groups in optimization can balance the performance of all classes. To this end, our approach executes the following training pipeline to obtain robust classifiers:

1. Cluster classes into groups with the help of initial validation performance based on the heuristic algorithm;
2. Evaluate the classifier’s performance on these groups based on updated model parameters;
3. Respectively update the groups’ weights and model parameters from learning losses;
4. The steps (2)/(3) loop until reaching the convergence.

Next, we report details on how to construct the distributionally robust surrogate loss function and schedule the group weights.

**Grouping classes in the imbalanced dataset.** First, we initially train the previously mentioned backbone model with the collected dataset in a standard supervised way, namely without any class imbalance suppression mechanism (such an initial training process is for empirically assessing the class imbalance circumstance). Then, based on the initial training results on the validation dataset, we adopt the clustering strategy as follows: (i) treat classes with nearly zero *F1-scores* as separate groups and (ii) cluster the remainder classes into other limited groups with the instance numbers for each class as input. Such a design pays more attention to hardly discriminating minority classes. Also, note that the results for the majority classes with similar training samples are close to each other in terms of initial training performance. In light of this, we leverage empirical assessment and observations as prior knowledge to define groups based on the training data heuristically.

Here, we take the CIC-IDS2017 dataset (Sharafaldin et al., 2018) as an example. For the minority classes whose *F1-scores* are 0 in the initial standard training, we set these classes as separate groups. For other classes, we use data clustering algorithms, such as the K-means (Lloyd, 1982), to group the classes with similar training sample numbers. The role of initial training is to serve the formal training as getting groups fixed. With the grouping mechanism applied, the training data comprises  $(\mathbf{x}, y, g)$  triplets, where  $g \in \mathcal{G} = \{1, 2, \dots, K\}$  represents the group label for each input feature  $\mathbf{x}$  and  $K$  is denoted as the number of groups which varies depending on the dataset.

**Group distributionally robust loss function.** The distribution of data points can be written as  $p(\mathbf{x}, y, g)$ . Given an integer  $K$  as the number of groups, we denote the assignment matrix by  $\Gamma \in \mathbb{R}^{K \times c}$ , in which  $\gamma_{k,c}$  equals 1 if the  $k$ -th group contains the  $c$ -th class and 0 otherwise. The

group number generally is smaller than the class number, i.e.,  $1 < K \leq \mathcal{C}$ . Thus, the loss for each group can be formulated by:

$$\mathcal{L}_G(D; \theta) = \Gamma \mathcal{L}_C(D; \theta), \quad (5)$$

where  $\mathcal{L}_G(D; \theta) = [\ell_g(D_1; \theta), \dots, \ell_g(D_K; \theta)]^\top \in \mathbb{R}^K$  is the loss vector at the group level, and its  $k$ -th element corresponds to the summation of intra-group losses  $\sum_{c=1}^C \gamma_{k,c} \ell(D_c; \theta)$ . Naturally, we expect the classification model to generalize well on average and the worst-case group. However, there are variations in the generalization gaps across groups, which result in the gap between average and worst-group test performances. To bridge the gap, we attempt to reduce training loss in the groups with larger generalization gaps. Concretely, we adopt the operation in (Cao et al., 2019; Sagawa et al., 2019) to obtain  $\mathbf{v}_G = [B/\sqrt{n_1}, \dots, B/\sqrt{n_K}]^\top = [v_1, \dots, v_K]^\top$ , where  $n_k$  is the group size for the  $k$ -th group and  $B$  the model calibration constant treated as a hyper-parameter. The scaling with  $1/\sqrt{n_k}$  reflects that small groups are more likely to overfit than large groups. By applying the group calibrations, the model is inclined to pay more attention to fitting the smaller groups.

**Iteratively estimating the groups' weights.** We produce groups' weights with the grouping mechanism described above. To balance different groups, we place the weights over groups  $\omega = [\omega_1, \dots, \omega_K]^\top \in \Delta_K$ , where  $\omega_k \geq 0$  is specific to the  $k$ -th group. In the proposed approach, intra-group classes share the same weight, while different groups possess various weights. That is,  $\eta_i = \eta_j = \omega_k$  when the  $i$ -th and  $j$ -th classes belong to the  $k$ -th group. Thus, the minimax optimization problem in Eq. (4) is further regularized as follow:

$$\max_{\omega \in \Delta_K} \min_{\theta \in \Theta} \mathcal{F}(\omega, \theta) := \mathbb{E}_{p(D)} \left\{ \omega^\top [\Gamma \mathcal{L}_C(D; \theta) + \mathbf{v}_G] \right\}. \quad (6)$$

The optimization problem in Eq. (6) can be interpreted as approximately solving a stochastic two-player zero-sum Stackelberg game  $\mathcal{SG} = \langle \mathcal{P}_L, \mathcal{P}_F; \{\omega \in \Delta_K\}, \{\theta \in \Theta\}; \mathcal{F}(\omega, \theta) \rangle$ . The two players sequentially compete to maximize separate utility functions in  $\mathcal{SG}$ , which can be characterized as

$$\mathcal{SG} : \omega^{(t)} = \underbrace{\arg \max_{\omega \in \Delta_K} \mathbb{E}_{p(D)} \left\{ \omega^\top [\Gamma \mathcal{L}_C(D; \theta^{(t)}) + \mathbf{v}_G] \right\}}_{\text{Leader Player}} \quad (7a)$$

$$\theta^{(t+1)} = \underbrace{\arg \min_{\theta \in \Theta} \mathbb{E}_{p(D)} \left\{ (\omega^{(t)})^\top [\Gamma \mathcal{L}_C(D; \theta) + \mathbf{v}_G] \right\}}_{\text{Follower Player}} \quad (7b)$$

As for approximately obtaining the above best responses, the update of  $\omega$  takes the following rule the same as that in (Sagawa et al., 2019). Let  $\omega^{(t)}$  be the vector of groups' weights under the model's parameters  $\theta^{(t)}$ , then the  $i$ -th element in  $\omega$  is updated in the  $t$ -th iteration by:

$$\omega_i^{(t)} = \frac{\omega_i^{(t-1)} \exp \left( \beta (\ell_g(D_i; \theta^{(t)}) + v_i) \right)}{\sum_{k=1}^K \omega_k^{(t-1)} \exp \left( \beta (\ell_g(D_k; \theta^{(t)}) + v_k) \right)}, \quad \forall i \in \{1, \dots, K\} \text{ and } \omega^{(t-1)} = [\omega_1^{(t-1)}, \dots, \omega_K^{(t-1)}]^\top, \quad (8)$$

where  $\ell_g(D_k; \theta^{(t)})$  is the last time evaluated performance for the class  $k$ , and  $\sum_{k=1}^K \omega_k^{(t-1)} = 1$ .  $\beta$  denotes the temperature hyper-parameter to control the scale of the loss value.

For the model parameters' update, we apply the stochastic gradient descent to  $\theta$  with the learning rate  $\epsilon$  and the sampled batch sample  $D \sim p(D)$ :

$$\theta^{(t+1)} = \theta^{(t)} - \epsilon \cdot \nabla_{\theta} \omega^{(t)^\top} \Gamma \mathcal{L}_C(D; \theta^{(t)}). \quad (9)$$

### 4.3. Solution Concepts in GDR-CIL

Next, we focus on another crucial question in this part: **What is the notion of the convergence point in the game?** In response to this question, we need to formulate the corresponding solution concept in  $\mathcal{SG}$ . Here, we induce the global Stackelberg equilibrium as the solution concept.

**Definition 1** (Global Stackelberg Equilibrium). Let  $(\omega_*, \theta_*) \in \Delta_K \times \Theta$  be the solution. With the leader  $\omega_* \in \Delta_K$  and the follower  $\theta_* \in \Theta$ ,  $(\omega_*, \theta_*)$  is called a *global Stackelberg equilibrium* if the following inequalities are satisfied,  $\forall \omega \in \Delta_K$  and  $\forall \theta \in \Theta$ ,

$$\inf_{\theta' \in \Theta} \mathcal{F}(\omega, \theta') \leq \mathcal{F}(\omega_*, \theta_*) \leq \mathcal{F}(\omega_*, \theta).$$

**Proposition 1** (Existence of Equilibrium). *Suppose that  $\Theta$  is compact, the global Stackelberg equilibrium of  $\mathcal{F}(\omega, \theta)$  always exists.*

**Proof.** Since  $\mathcal{F}(\omega, \theta)$  is continuous with respect to  $\omega$  and  $\theta$ , along with that  $\Delta_K \in \mathbb{R}^K$  and  $\Theta$  are compact, Proposition 1 holds due to the extreme-value theorem. ■

We can further explain the obtained equilibrium  $(\omega_*, \theta_*)$  in a more intuitive way. That is, the leader has already specified the optimal strategy  $\omega_*$  for reweighting different groups, while the follower cannot find another model parameter except  $\theta_*$  to minimize the negative effect of class imbalance in the worst groups. As a result, we can obtain a robust class imbalance learner from the devised optimization strategies.

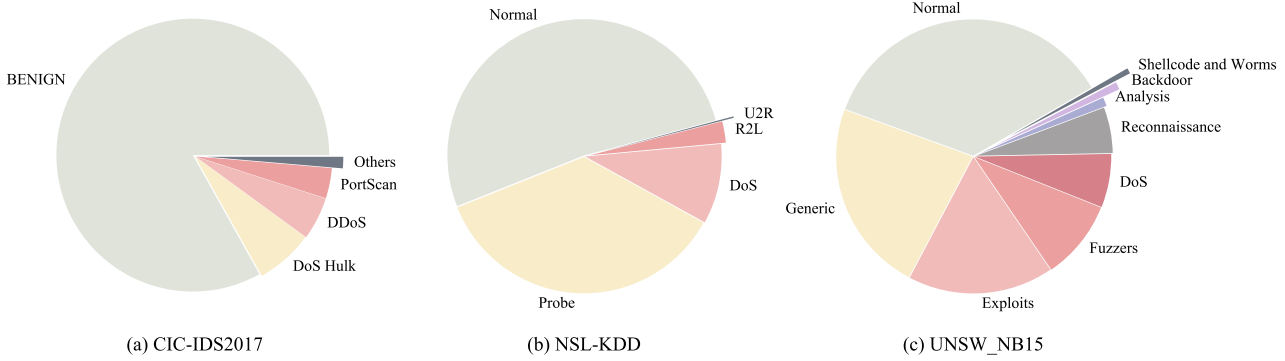


Figure 2. Data volumes for each class of the three datasets. In panel (a), “Others” contains 11 minority classes, which are DoS GoldenEye, FTP-Patator, DoS slowloris, DoS slowhttptest, SSH-Patator, Bot, Web Attack Brute Force, Web Attack XSS, Infiltration, Web Attack Sql Injection and Heartbleed, each of them accounting for less than 0.5% of CIC-IDS2017 dataset.

#### Algorithm 1 Training Processes in **GDR-CIL** Methods.

```

1: Input: Maximum iteration number  $T$ ; Batch size  $N_b$ ;
   Learning rate  $\epsilon$ ; Temperature hyper-parameter  $\beta$ ; Group
   number  $K$ ; Group size for the  $K$  groups  $n_1, \dots, n_K$ ;
   Assignment matrix  $\Gamma$ ; Calibration hyper-parameter  $B$ ;
   Class number  $\mathcal{C}$ ; Weight vector  $\omega$ .
2: Initialize model parameters  $\theta^{(1)}$ ;
3: Initialize each group weight  $\omega_k^{(0)} \leftarrow \frac{1}{K}$ ;
4: Compute the calibration vector  $\mathbf{v}_g = [B/\sqrt{n_1}, \dots, B/\sqrt{n_K}]^\top$ ;
5: for  $t = 1 : T$  do
6:   Randomly sample a batch of training samples:
       $D^{(t)} := \{(\mathbf{x}_n, y_n, g_n)\}_{n=1}^{N_b}$ , where  $\mathbf{x}_n \in \mathcal{X}, y_n \in \mathcal{Y}, g_n \in \mathcal{G}$ ;
7:   Compute the empirical risk for each class at  $t$ -th
      iteration  $\mathcal{L}_{\mathcal{C}}(D^{(t)}; \theta^{(t)})$ ;
8:   Compute the group risk  $\mathcal{L}_{\mathcal{G}}(D^{(t)}; \theta^{(t)})$  in Eq. (5)
      with the help of  $\Gamma$ ;
9:   # The Leader's Decision-Making
10:  Estimate group weights  $\omega^{(t)}(\theta^{(t)})$  according to Eq.
      (8),  $\omega^{(t-1)}$  and  $\mathcal{L}_{\mathcal{G}}(D^{(t)}; \theta^{(t)})$ ;
11:  # The Follower's Decision-Making
12:  Update the model parameters to obtain  $\theta^{(t+1)}$  by
      applying the stochastic gradient descent with the learn-
      ing rate  $\epsilon$  and  $\omega^{(t)}$  according to Eq. (9).
13: end for

```

## 5. Experimental Results and Analysis

This section starts with the commonly-seen benchmarks and baselines in class imbalance network traffic classification, conducts extensive experiments, and performs quantitative analysis.

### 5.1. Experimental Settings

Here, we present the benchmarks, baselines, and evaluation metrics used in this work.

**Benchmarks:** Three typical datasets are used to examine the performance of the proposed method, including CIC-IDS2017 (Sharafaldin et al., 2018), NSL-KDD (Tavallaei et al., 2009) and UNSW-NB15 datasets (Moustafa & Slay, 2015). Please refer to Appendix A for details.

Figure 2 displays the data volumes for each class of the three datasets. It can be seen that the traffic data categories are extremely imbalanced in these datasets.

**Baselines:** Deep imbalanced learning is considered for network traffic classification. Here, we compare **GDR-CIL** with typical and state-of-the-art (SOTA) baselines achieved by various strategies. They include expected risk minimization (ERM) loss, Focal loss (Lin et al., 2017), CB (Cui et al., 2019), Mixup-DRW (Zhang et al., 2017), Remix-DRW (Chou et al., 2020), LDAM-DRW (Cao et al., 2019), and LDR-KL (Zhu et al., 2023a). We refer the reader to Appendix B for more details on these baselines.

**Evaluation Metrics:** Three classical evaluation indicators are used to evaluate the performance of all methods in the experiment: (1) *Specificity* is the true negative rate, measuring the proportion of actual negative samples correctly predicted as negative. (2) *F1-score* takes the harmonic mean of another two performance metrics, namely *Precision* and *Recall*, to balance performance. (3) *G-mean* is the geometric mean of *Specificity* and *Recall*.

The above comprehensive indicators are derived from four basic metrics obtained from the classification model, which are True Positive (TP), False Positive (FP), True Negative (TN), and False Negative (FN) in the confusion matrix. This work considers multiclass network traffic classification;

hence, samples from one specific traffic class are treated as positive, with others as negative in evaluation. Here, the TP and TN represent the number of positive and negative samples that are correctly classified, respectively. The FP indicates the number of negative samples misclassified as positive, while the FN counts the number of positive samples misclassified as negative.

We calculate *Recall* and *Precision* from the basic metrics,  $Recall = TP / (TP + FN)$  and  $Precision = TP / (TP + FP)$ . The resulting comprehensive indicators are further obtained from the operations:

$$Specificity = \frac{TN}{TN + FP}, \quad (10)$$

$$F1\text{-score} = \frac{2 \times Recall \times Precision}{Recall + Precision}, \quad (11)$$

$$G\text{-mean} = \sqrt{Recall \times Specificity}. \quad (12)$$

Note that these indicators *F1-score*, *Specificity*, and *G-mean* are always positively related to the class imbalance performance.

**Implementation Details:** We randomly split the dataset into standard training-validation-testing datasets. The validation dataset works for hyper-parameter configurations in the training process, and the testing dataset is used to evaluate experimental results. For the sake of generality, we employ a multi-layer perception (MLP) as the backbone of deep neural networks. It is a fully connected neural network with two hidden layers, and we use ReLU as the activation function. We optimized the neural network using stochastic gradient descent with a learning rate of  $1e - 2$  and a weight decay of  $1e - 4$ . Please refer to Appendix C for details.

## 5.2. Experimental Results

In the field of imbalance network traffic classification, comprehensive indicators are commonly used in performance evaluation. Hence, we respectively report comprehensive indicators, such as *Specificity*, *F1-score*, *G-mean* on all benchmarks' testing datasets using various classification models.

**Result analysis from *Specificity*.** Figure 3 indicates the *Specificity* comparisons between **GDR-CIL** and the other seven baselines. **GDR-CIL** surpasses all other baselines on the two extremely imbalanced datasets, CIC-IDS2017 and UNSW-NB15. For the NSL-KDD dataset, a less imbalanced dataset with only five classes, the grouping mechanism in **GDR-CIL** encounters limitations in improving performance. As a result, **GDR-CIL** exhibits a slight degradation in the average *Specificity*.

**Result analysis from *F1-score*.** As observed in Table 1, all baselines except ours achieve relatively high average

performance on *F1-score* for all majority and some minority classes on CIC-IDS2017 dataset. However, most of them yield low *F1-scores* in certain minority classes, such as “Web Attack XSS” class where the *F1-score* is almost 0. In comparison, **GDR-CIL**’s performance is comparable to other baseline methods on major classes while retaining discriminative capability for the minority classes. Particularly, in minor but more risky classes like “Web Attack XSS”, “Infiltration” and “Web Attack Sql Injection”, our approach exhibits a significant improvement over several baselines which achieve *F1-scores* nearly 0, e.g., notably increasing the score by at least 31.87% in “Web Attack XSS” class over LDAW-DRW.

Note that LDAM-DRW exhibits a subtle ability to recognize all minority classes benefiting from class-dependent margin constraint, while **GDR-CIL** enhances the recognition performance for hard-to-classify minority classes by reweighting losses at the group level. Additionally, **GDR-CIL** outperforms all baselines in average *F1-score*, illustrating its strength in mitigating the negative effect of class imbalance. The above evidence underscores the necessity of employing group distributionally robust optimization in addressing network traffic classification with numerous minority classes.

For NSL-KDD and UNSW-NB15 datasets with less minority classes, we report the *F1-scores* in Tables 2/3. On the NSL-KDD dataset, the baselines ERM, Mixup-DRW, Remix-DRW, and LDR-KL exhibit no identification capability for the minority class “U2R”, resulting in *F1-score* = 0. The remaining baselines cannot achieve *F1-scores* higher than 41%. In contrast, **GDR-CIL** still obtains nearly 49.19% *F1-score* on the minority class “U2R” and simultaneously retains comparable performance to other baselines on four majority classes. On the UNSW-NB15 dataset, **GDR-CIL** beats all baselines on average *F1-score*, likely attributed to its remarkable performance gains in the minority class “backdoor”.

**Result analysis from *G-mean*.** Tables 4-6 illustrate the phenomenon similar to that of collected results in *F1-score* in statistics. Without sacrificing too much identification of the majority classes, **GDR-CIL** consistently outperforms all other baselines in terms of average *G-means* for most minority classes. This further examines the significance of group distributionally robust optimization in suppressing the negative influence of class imbalance.

## 5.3. Ablation Studies

Our ablation studies are to examine: (1) The extent of performance improvement achieved by using the grouping mechanism as compared to not using it; (2) The feasibility of the heuristic estimate of the number of groups; (3) The impact of the hyper-parameters in **GDR-CIL** on the multi-classification performance. Without loss of generality, we

Table 1. **F1-scores obtained by different methods on CIC-IDS2017 dataset (5 runs).** Underlined traffic categories belong to the minority class. The results are expressed in % with standard deviations.

Traffic Category	ERM	Focal	CB-SGM	Mixup-DRW	Remix-DRW	LDAM-DRW	LDR-KL	GDR-CIL (Ours)
BENIGN	<b>97.51<math>\pm</math>0.05</b>	97.33 $\pm$ 0.04	97.32 $\pm$ 0.03	97.48 $\pm$ 0.05	97.47 $\pm$ 0.03	97.07 $\pm$ 0.35	97.39 $\pm$ 0.10	94.94 $\pm$ 0.06
DoS Hulk	95.62 $\pm$ 0.46	94.18 $\pm$ 0.39	95.03 $\pm$ 0.34	95.61 $\pm$ 0.45	95.59 $\pm$ 0.39	94.74 $\pm$ 0.37	<b>96.05<math>\pm</math>0.29</b>	91.68 $\pm$ 0.08
DDoS	98.50 $\pm$ 0.04	98.09 $\pm$ 0.07	97.55 $\pm$ 0.06	98.5 $\pm$ 0.11	98.46 $\pm$ 0.02	98.43 $\pm$ 0.10	<b>98.91<math>\pm</math>0.03</b>	95.02 $\pm$ 0.10
PortScan	91.42 $\pm$ 0.02	91.15 $\pm$ 0.10	91.31 $\pm$ 0.05	91.42 $\pm$ 0.02	91.44 $\pm$ 0.01	<b>91.50<math>\pm</math>0.04</b>	89.81 $\pm$ 0.90	90.22 $\pm$ 0.11
DoS GoldenEye	98.61 $\pm$ 0.04	98.30 $\pm$ 0.01	98.40 $\pm$ 0.03	98.56 $\pm$ 0.03	98.48 $\pm$ 0.04	96.93 $\pm$ 0.09	<b>98.78<math>\pm</math>0.02</b>	97.06 $\pm$ 0.07
<u>FTP-Patator</u>	97.89 $\pm$ 0.05	98.11 $\pm$ 0.10	97.7 $\pm$ 0.03	97.85 $\pm$ 0.03	97.76 $\pm$ 0.05	98.11 $\pm$ 0.17	<b>98.49<math>\pm</math>0.10</b>	97.44 $\pm$ 0.03
<u>DoS slowloris</u>	97.03 $\pm$ 0.06	<b>97.53<math>\pm</math>0.12</b>	96.06 $\pm$ 0.16	96.85 $\pm$ 0.08	96.77 $\pm$ 0.06	96.43 $\pm$ 0.29	96.89 $\pm$ 0.18	95.30 $\pm$ 0.14
DoS Slowhttptest	98.23 $\pm$ 0.02	<b>98.34<math>\pm</math>0.03</b>	97.70 $\pm$ 0.02	98.26 $\pm$ 0.04	98.26 $\pm$ 0.02	98.19 $\pm$ 0.03	98.24 $\pm$ 0.03	97.74 $\pm$ 0.05
<u>SSH-Patator</u>	94.72 $\pm$ 0.03	94.88 $\pm$ 0.24	94.14 $\pm$ 0.02	94.58 $\pm$ 0.09	94.42 $\pm$ 0.08	95.11 $\pm$ 0.22	95.24 $\pm$ 0.17	<b>95.50<math>\pm</math>0.00</b>
Bot	<b>77.48<math>\pm</math>0.06</b>	76.08 $\pm$ 0.70	74.47 $\pm$ 0.05	77.29 $\pm$ 0.07	77.17 $\pm$ 0.20	73.20 $\pm$ 3.53	76.77 $\pm$ 2.30	55.72 $\pm$ 0.60
Web Attack Brute Force	69.03 $\pm$ 0.03	69.88 $\pm$ 0.46	69.00 $\pm$ 0.13	69.05 $\pm$ 0.03	69.05 $\pm$ 0.05	59.61 $\pm$ 9.50	<b>70.44<math>\pm</math>0.37</b>	39.08 $\pm$ 2.02
Web Attack XSS	0.00 $\pm$ 0.00	0.00 $\pm$ 0.00	0.00 $\pm$ 0.00	0.00 $\pm$ 0.00	0.00 $\pm$ 0.00	9.26 $\pm$ 7.29	0.00 $\pm$ 0.00	<b>41.13<math>\pm</math>3.73</b>
<u>Infiltration</u>	0.00 $\pm$ 0.00	0.00 $\pm$ 0.00	16.91 $\pm$ 4.28	0.00 $\pm$ 0.00	0.00 $\pm$ 0.00	1.77 $\pm$ 1.58	0.00 $\pm$ 0.00	<b>36.31<math>\pm</math>0.99</b>
Web Attack Sql Injection	0.00 $\pm$ 0.00	0.00 $\pm$ 0.00	0.00 $\pm$ 0.00	0.00 $\pm$ 0.00	0.00 $\pm$ 0.00	0.19 $\pm$ 0.17	0.00 $\pm$ 0.00	<b>6.62<math>\pm</math>0.71</b>
Heartbleed	0.00 $\pm$ 0.00	45.0 $\pm$ 16.43	73.33 $\pm$ 1.49	0.00 $\pm$ 0.00	30.0 $\pm$ 16.43	79.44 $\pm$ 2.56	0.00 $\pm$ 0.00	<b>80.89<math>\pm</math>3.64</b>
<b>Average</b> $\uparrow$	67.74 $\pm$ 0.09	70.59 $\pm$ 2.63	73.26 $\pm$ 0.36	67.7 $\pm$ 0.08	69.66 $\pm$ 2.49	72.77 $\pm$ 0.32	67.80 $\pm$ 0.22	<b>74.31<math>\pm</math>0.49</b>

Table 2. **F1-scores obtained by different methods on NSL-KDD dataset (5 runs).** The underlined traffic category belongs to the minority class. The results are expressed in % with standard deviations.

Traffic Category	ERM	Focal	CB-SGM	Mixup-DRW	Remix-DRW	LDAM-DRW	LDR-KL	GDR-CIL (Ours)
Normal	<b>99.27<math>\pm</math>0.02</b>	99.16 $\pm$ 0.02	99.23 $\pm$ 0.01	99.24 $\pm$ 0.01	99.23 $\pm$ 0.01	<b>99.27<math>\pm</math>0.03</b>	99.08 $\pm$ 0.02	97.82 $\pm$ 0.03
Probe	<b>96.69<math>\pm</math>0.04</b>	96.42 $\pm$ 0.04	96.56 $\pm$ 0.04	96.66 $\pm$ 0.05	96.60 $\pm$ 0.02	96.47 $\pm$ 0.30	96.63 $\pm$ 0.03	94.76 $\pm$ 0.04
DoS	97.29 $\pm$ 0.02	97.26 $\pm$ 0.05	97.32 $\pm$ 0.04	97.37 $\pm$ 0.07	97.26 $\pm$ 0.07	<b>97.38<math>\pm</math>0.09</b>	97.23 $\pm$ 0.04	96.34 $\pm$ 0.08
R2L	90.00 $\pm$ 0.18	89.53 $\pm$ 0.11	89.43 $\pm$ 0.12	89.84 $\pm$ 0.13	89.83 $\pm$ 0.11	<b>90.27<math>\pm</math>0.38</b>	89.85 $\pm$ 0.04	87.89 $\pm$ 0.12
U2R	0.00 $\pm$ 0.00	3.41 $\pm$ 1.87	40.07 $\pm$ 9.03	0.00 $\pm$ 0.00	0.00 $\pm$ 0.00	35.66 $\pm$ 10.34	0.00 $\pm$ 0.00	<b>49.19<math>\pm</math>0.34</b>
<b>Average</b> $\uparrow$	76.65 $\pm$ 0.11	77.15 $\pm$ 0.85	84.52 $\pm$ 1.80	76.62 $\pm$ 0.11	76.58 $\pm$ 0.08	83.81 $\pm$ 2.16	76.56 $\pm$ 0.03	<b>85.20<math>\pm</math>0.08</b>

Table 3. **F1-scores obtained by different methods on UNSW-NB15 dataset (5 runs).** Underlined traffic categories belong to the minority class. The results are expressed in % with standard deviations.

Traffic Category	ERM	Focal	CB-SGM	Mixup-DRW	Remix-DRW	LDAM-DRW	LDR-KL	GDR-CIL (Ours)
Normal	98.53 $\pm$ 0.02	98.53 $\pm$ 0.02	98.54 $\pm$ 0.02	98.54 $\pm$ 0.01	98.52 $\pm$ 0.01	<b>98.57<math>\pm</math>0.00</b>	98.53 $\pm$ 0.02	98.54 $\pm$ 0.01
Generic	82.87 $\pm$ 0.05	82.84 $\pm$ 0.03	82.88 $\pm$ 0.04	<b>82.94<math>\pm</math>0.07</b>	<b>82.94<math>\pm</math>0.03</b>	82.74 $\pm$ 0.02	82.81 $\pm$ 0.05	82.71 $\pm$ 0.01
Exploits	77.35 $\pm$ 0.15	77.69 $\pm$ 0.27	76.83 $\pm$ 0.39	76.69 $\pm$ 0.24	77.01 $\pm$ 0.21	78.40 $\pm$ 0.11	<b>79.32<math>\pm</math>0.10</b>	77.08 $\pm$ 0.27
Fuzzers	74.40 $\pm$ 0.10	74.44 $\pm$ 0.12	74.45 $\pm$ 0.12	74.34 $\pm$ 0.06	74.40 $\pm$ 0.04	74.21 $\pm$ 0.03	<b>74.62<math>\pm</math>0.05</b>	73.82 $\pm$ 0.26
DoS	58.17 $\pm$ 0.15	58.05 $\pm$ 0.08	58.04 $\pm$ 0.17	57.97 $\pm$ 0.15	58.08 $\pm$ 0.05	58.16 $\pm$ 0.11	<b>58.54<math>\pm</math>0.09</b>	58.05 $\pm$ 0.12
Reconnaissance	56.76 $\pm$ 0.09	56.87 $\pm$ 0.16	56.57 $\pm$ 0.06	56.58 $\pm$ 0.10	56.48 $\pm$ 0.04	<b>57.25<math>\pm</math>0.14</b>	57.14 $\pm$ 0.22	55.84 $\pm$ 0.24
Analysis	31.83 $\pm$ 0.15	31.53 $\pm$ 0.24	32.03 $\pm$ 0.1	31.73 $\pm$ 0.17	31.61 $\pm$ 0.18	32.54 $\pm$ 0.14	<b>32.59<math>\pm</math>0.15</b>	27.77 $\pm$ 0.06
Backdoor	0.00 $\pm$ 0.00	1.37 $\pm$ 0.76	0.00 $\pm$ 0.00	0.00 $\pm$ 0.00	0.00 $\pm$ 0.00	0.06 $\pm$ 0.05	0.00 $\pm$ 0.00	<b>23.17<math>\pm</math>0.28</b>
Shellcode	38.54 $\pm$ 0.21	41.64 $\pm$ 1.15	38.02 $\pm$ 0.46	37.71 $\pm$ 0.42	38.46 $\pm$ 0.57	43.76 $\pm$ 1.25	<b>45.82<math>\pm</math>0.93</b>	45.23 $\pm$ 0.94
Worms	5.28 $\pm$ 4.73	15.67 $\pm$ 5.73	19.79 $\pm$ 4.46	6.15 $\pm$ 4.59	10.38 $\pm$ 5.69	<b>22.51<math>\pm</math>1.42</b>	0.00 $\pm$ 0.00	21.61 $\pm$ 0.57
<b>Average</b> $\uparrow$	52.37 $\pm$ 1.17	53.86 $\pm$ 0.68	53.71 $\pm$ 1.11	52.26 $\pm$ 1.16	52.79 $\pm$ 1.42	54.82 $\pm$ 0.26	52.94 $\pm$ 0.30	<b>56.38<math>\pm</math>0.23</b>

Table 4. **G-means obtained by different methods on CIC-IDS2017 dataset (5 runs).** Underlined traffic categories belong to the minority class. The results are expressed in % with standard deviations.

Traffic Category	ERM	Focal	CB-SGM	Mixup-DRW	Remix-DRW	LDAM-DRW	LDR-KL	GDR-CIL (Ours)
BENIGN	<b>96.88<math>\pm</math>0.07</b>	96.67 $\pm$ 0.04	96.62 $\pm$ 0.05	96.86 $\pm$ 0.07	96.86 $\pm$ 0.05	96.57 $\pm$ 0.29	96.64 $\pm$ 0.17	94.83 $\pm$ 0.06
DoS Hulk	96.44 $\pm$ 0.40	95.71 $\pm$ 0.23	95.99 $\pm$ 0.32	96.38 $\pm$ 0.42	96.63 $\pm$ 0.39	<b>96.93<math>\pm</math>0.05</b>	96.6 $\pm$ 0.28	96.18 $\pm$ 0.03
DDoS	98.82 $\pm$ 0.03	98.54 $\pm$ 0.05	98.41 $\pm$ 0.03	98.84 $\pm$ 0.09	98.81 $\pm$ 0.02	98.84 $\pm$ 0.07	<b>99.19<math>\pm</math>0.02</b>	97.00 $\pm$ 0.07
PortScan	<b>99.24<math>\pm</math>0.00</b>	99.22 $\pm$ 0.01	99.03 $\pm$ 0.05	99.23 $\pm$ 0.00	99.24 $\pm$ 0.00	<b>99.24<math>\pm</math>0.00</b>	97.12 $\pm$ 0.91	98.81 $\pm$ 0.10
DoS GoldenEye	99.26 $\pm$ 0.04	99.21 $\pm$ 0.00	99.18 $\pm$ 0.02	99.25 $\pm$ 0.03	99.21 $\pm$ 0.00	99.23 $\pm$ 0.20	<b>99.47<math>\pm</math>0.00</b>	98.68 $\pm$ 0.02
FTP-Patator	99.65 $\pm$ 0.00	<b>99.67<math>\pm</math>0.00</b>	99.64 $\pm$ 0.01	99.65 $\pm$ 0.00	99.65 $\pm$ 0.01	99.58 $\pm$ 0.02	99.64 $\pm$ 0.02	99.67 $\pm$ 0.01
DoS slowloris	97.85 $\pm$ 0.00	<b>98.13<math>\pm</math>0.14</b>	97.29 $\pm$ 0.14	97.86 $\pm$ 0.01	97.88 $\pm$ 0.02	97.89 $\pm$ 0.03	97.94 $\pm$ 0.11	97.85 $\pm$ 0.04
DoS Slowhttptest	99.19 $\pm$ 0.01	<b>99.22<math>\pm</math>0.01</b>	98.91 $\pm$ 0.01	99.18 $\pm$ 0.02	99.17 $\pm$ 0.02	99.14 $\pm$ 0.03	99.20 $\pm$ 0.01	99.14 $\pm$ 0.02
SSH-Patator	95.63 $\pm$ 0.00	95.63 $\pm$ 0.00	95.62 $\pm$ 0.00	95.64 $\pm$ 0.01	95.64 $\pm$ 0.01	<b>95.65<math>\pm</math>0.01</b>	95.64 $\pm$ 0.00	<b>95.65<math>\pm</math>0.00</b>
Bot	81.62 $\pm$ 0.03	80.25 $\pm$ 0.71	78.15 $\pm$ 0.04	81.58 $\pm$ 0.02	81.41 $\pm$ 0.17	84.87 $\pm$ 2.98	81.11 $\pm$ 0.24	<b>98.91<math>\pm</math>0.04</b>
Web Attack Brute Force	92.31 $\pm$ 0.00	93.15 $\pm$ 0.50	92.04 $\pm$ 0.11	92.32 $\pm$ 0.00	92.32 $\pm$ 0.00	81.04 $\pm$ 10.98	<b>93.41<math>\pm</math>0.42</b>	76.45 $\pm$ 3.51
Web Attack XSS	0.00 $\pm$ 0.00	0.00 $\pm$ 0.00	0.00 $\pm$ 0.00	0.00 $\pm$ 0.00	0.00 $\pm$ 0.00	22.20 $\pm$ 16.63	0.00 $\pm$ 0.00	<b>77.34<math>\pm</math>6.87</b>
Infiltration	0.00 $\pm$ 0.00	0.00 $\pm$ 0.00	28.02 $\pm$ 6.55	0.00 $\pm$ 0.00	0.00 $\pm$ 0.00	17.69 $\pm$ 15.82	0.00 $\pm$ 0.00	<b>72.65<math>\pm</math>1.07</b>
Web Attack Sql Injection	0.00 $\pm$ 0.00	0.00 $\pm$ 0.00	0.00 $\pm$ 0.00	0.00 $\pm$ 0.00	0.00 $\pm$ 0.00	8.93 $\pm$ 7.98	0.00 $\pm$ 0.00	<b>59.51<math>\pm</math>3.31</b>
Heartbleed	0.00 $\pm$ 0.00	<b>46.48<math>\pm</math>16.97</b>	77.46 $\pm$ 0.00	0.00 $\pm$ 0.00	30.98 $\pm$ 16.97	84.36 $\pm$ 4.07	0.00 $\pm$ 0.00	<b>89.44<math>\pm</math>0.00</b>
<b>Average <math>\uparrow</math></b>	70.46 $\pm$ 0.03	73.46 $\pm$ 1.21	77.09 $\pm$ 0.42	70.45 $\pm$ 0.04	72.52 $\pm$ 1.15	78.81 $\pm$ 2.35	70.4 $\pm$ 0.09	<b>90.14<math>\pm</math>0.43</b>

Table 5. **G-means obtained by different methods on NSL-KDD dataset (5 runs).** The underlined traffic category belongs to the minority class. The results are expressed in % with standard deviations.

Traffic Category	ERM	Focal	CB-SGM	Mixup-DRW	Remix-DRW	LDAM-DRW	LDR-KL	GDR-CIL (Ours)
Normal	99.38 $\pm$ 0.01	99.32 $\pm$ 0.01	99.35 $\pm$ 0.01	99.37 $\pm$ 0.01	99.36 $\pm$ 0.01	<b>99.41<math>\pm</math>0.03</b>	99.26 $\pm$ 0.02	97.97 $\pm$ 0.02
Probe	<b>97.08<math>\pm</math>0.04</b>	96.80 $\pm$ 0.04	96.96 $\pm$ 0.04	97.06 $\pm$ 0.05	97.01 $\pm$ 0.02	96.79 $\pm$ 0.31	97.03 $\pm$ 0.04	95.37 $\pm$ 0.04
DoS	98.92 $\pm$ 0.01	<b>99.00<math>\pm</math>0.02</b>	98.91 $\pm$ 0.02	98.94 $\pm$ 0.01	98.90 $\pm$ 0.02	<b>99.00<math>\pm</math>0.05</b>	98.92 $\pm$ 0.02	98.50 $\pm$ 0.07
R2L	95.63 $\pm$ 0.06	95.97 $\pm$ 0.07	94.98 $\pm$ 0.10	95.38 $\pm$ 0.09	95.43 $\pm$ 0.06	96.29 $\pm$ 0.07	95.22 $\pm$ 0.18	<b>96.94<math>\pm</math>0.07</b>
U2R	0.00 $\pm$ 0.00	8.53 $\pm$ 4.67	56.51 $\pm$ 12.67	0.00 $\pm$ 0.00	0.00 $\pm$ 0.00	60.48 $\pm$ 13.80	0.00 $\pm$ 0.00	<b>73.81<math>\pm</math>0.00</b>
<b>Average <math>\uparrow</math></b>	78.20 $\pm$ 0.02	79.92 $\pm$ 0.94	89.34 $\pm$ 2.53	78.15 $\pm$ 0.02	78.14 $\pm$ 0.01	90.40 $\pm$ 2.75	78.08 $\pm$ 0.03	<b>92.52<math>\pm</math>0.02</b>

Table 6. **G-means obtained by different methods on UNSW-NB15 dataset (5 runs).** Underlined traffic categories belong to the minority class. The results are expressed in % with standard deviations.

Traffic Category	ERM	Focal	CB-SGM	Mixup-DRW	Remix-DRW	LDAM-DRW	LDR-KL	GDR-CIL (Ours)
Normal	<b>98.71<math>\pm</math>0.00</b>	98.70 $\pm$ 0.00	98.7 $\pm$ 0.00	98.70 $\pm$ 0.00	98.7 $\pm$ 0.00	<b>98.71<math>\pm</math>0.00</b>	<b>98.71<math>\pm</math>0.00</b>	98.69 $\pm$ 0.00
Generic	84.34 $\pm$ 0.04	84.30 $\pm$ 0.04	84.37 $\pm$ 0.07	<b>84.41<math>\pm</math>0.09</b>	84.39 $\pm$ 0.04	84.07 $\pm$ 0.01	84.16 $\pm$ 0.09	83.97 $\pm$ 0.01
Exploits	86.79 $\pm$ 0.08	86.95 $\pm$ 0.13	86.59 $\pm$ 0.11	86.68 $\pm$ 0.03	86.80 $\pm$ 0.06	87.06 $\pm$ 0.06	<b>87.38<math>\pm</math>0.04</b>	86.10 $\pm$ 0.22
Fuzzers	87.87 $\pm$ 0.07	87.74 $\pm$ 0.09	87.82 $\pm$ 0.07	87.71 $\pm$ 0.07	87.75 $\pm$ 0.07	87.65 $\pm$ 0.04	<b>87.91<math>\pm</math>0.04</b>	85.89 $\pm$ 0.21
DoS	68.73 $\pm$ 0.12	68.71 $\pm$ 0.14	68.78 $\pm$ 0.16	68.79 $\pm$ 0.11	68.88 $\pm$ 0.07	68.52 $\pm$ 0.17	<b>68.95<math>\pm</math>0.18</b>	68.47 $\pm$ 0.17
Reconnaissance	80.03 $\pm$ 0.08	80.13 $\pm$ 0.16	79.80 $\pm$ 0.05	79.76 $\pm$ 0.09	79.74 $\pm$ 0.03	80.61 $\pm$ 0.14	<b>80.66<math>\pm</math>0.29</b>	77.90 $\pm$ 0.38
Analysis	52.85 $\pm$ 0.29	52.49 $\pm$ 0.33	53.35 $\pm$ 0.18	52.84 $\pm$ 0.30	52.45 $\pm$ 0.33	54.33 $\pm$ 0.24	<b>54.51<math>\pm</math>0.20</b>	44.82 $\pm$ 0.10
Backdoor	0.00 $\pm$ 0.00	5.44 $\pm$ 3.00	0.00 $\pm$ 0.00	0.00 $\pm$ 0.00	0.00 $\pm$ 0.00	0.74 $\pm$ 0.67	0.00 $\pm$ 0.00	<b>50.86<math>\pm</math>0.53</b>
Shellcode	54.47 $\pm$ 0.70	56.95 $\pm$ 0.76	52.82 $\pm$ 0.95	52.47 $\pm$ 0.81	53.42 $\pm$ 0.90	59.66 $\pm$ 1.09	59.36 $\pm$ 0.83	<b>67.92<math>\pm</math>0.73</b>
Worms	7.89 $\pm$ 7.06	23.66 $\pm$ 8.64	31.55 $\pm$ 7.05	10.87 $\pm$ 6.89	15.78 $\pm$ 8.64	37.51 $\pm$ 1.72	0.00 $\pm$ 0.00	<b>39.43<math>\pm</math>0.00</b>
<b>Average <math>\uparrow</math></b>	62.17 $\pm$ 0.78	64.51 $\pm$ 1.12	64.38 $\pm$ 0.78	62.22 $\pm$ 0.74	62.79 $\pm$ 0.94	65.89 $\pm$ 0.31	62.16 $\pm$ 0.11	<b>70.41<math>\pm</math>0.09</b>

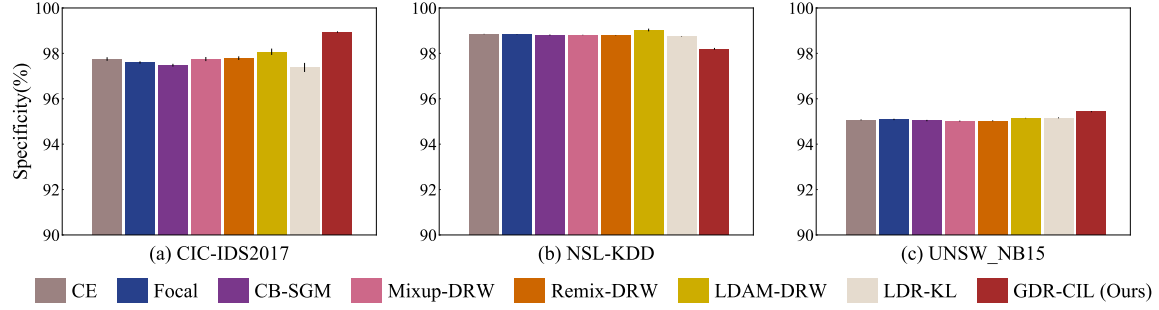


Figure 3. The average *Specificities* of different methods on three datasets (5 runs with error bars reported).

conduct these experiments on CIC-IDS2017 dataset.

Table 7. Influence of grouping in **GDR-CIL** on CIC-IDS2017 dataset (5 runs). The results are expressed in % with standard deviations.

	<i>F1-score</i> $\uparrow$	<i>G-mean</i> $\uparrow$	<i>Specificity</i> $\uparrow$
Non-grouped	70.41 $\pm$ 0.35	83.01 $\pm$ 0.17	99.39 $\pm$ 0.02
$K = 8, B = 0$	72.55 $\pm$ 0.37	84.02 $\pm$ 0.65	99.44 $\pm$ 0.01
$K = 8, B = 0.25$	74.31 $\pm$ 0.49	90.14 $\pm$ 0.43	99.44 $\pm$ 0.01

**Effectiveness of the Grouping Mechanism.** To better understand the role of class clusters, we perform an ablation study by removing the grouping operation in the loss function. The resulting non-grouped **GDR-CIL** treats each class as a separate group. We also take an interest in the calibration  $\mathbf{v}_G$  with a hyper-parameter  $B$ . Table 7 compares the grouped **GDR-CIL** and the non-grouped **GDR-CIL** in all comprehensive indicators. We can observe that the two grouped **GDR-CILs** with  $B = 0$  and  $B = 0.25$  are overall superior to the non-grouped one. This suggests that the grouping mechanism tends to focus more on the minority classes and correct the decision bias in the imbalanced case.

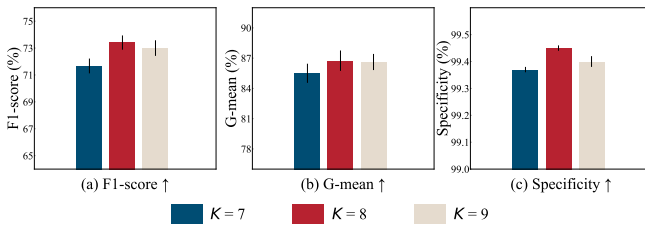


Figure 4. The comprehensive performance of **GDR-CIL** with error bars by varying the number of groups on CIC-IDS2017 dataset (5 runs).

**Feasibility of Heuristic Group Number Estimates.** We conduct experiments by varying the number of groups  $K$  to assess its impact on performance. Since different cluster numbers in the K-means algorithm lead to varying group

numbers, we evaluate the classification performance under different group numbers by adjusting the number of clusters. Specifically,  $K = 7, 8$  and  $9$  are investigated. Figure 4 shows the comparison results of **GDR-CIL**, in which we empirically set  $B = 0.25$  and  $\beta = 0.005$ . It reveals the necessity of appropriate selection of the group number, but nearly all cases still reserve superiority over other baseline results in Table 1.

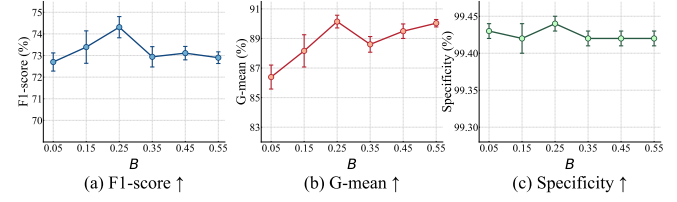


Figure 5. The comprehensive performance of **GDR-CIL** with error bars by varying  $B$  values on CIC-IDS2017 dataset (5 runs).

**Calibration Hyper-parameter  $B$  Study.** One hyper-parameter in the grouping mechanism is the calibration vector  $\mathbf{v}_G$ , where  $B$  controls its scale in  $\mathbf{v}_G = [B/\sqrt{n_1}, \dots, B/\sqrt{n_K}]^T$ . Here, we set  $K = 8$  and  $\beta = 0.005$ , which has been proven to achieve the best performance in other experiments. As revealed in Figure 5, *F1-score* and *G-mean* values rise with the increase of  $B$  from 0.05 to 0.25, with highest results at  $B = 0.25$ . The *Specificities* are close at each point with the best result at  $B = 0.25$ . Although *G-mean* tends to increase after  $B = 0.35$ , the overall best performance is at  $B = 0.25$ .

**Temperature Hyper-parameter  $\beta$  Study.** Another relevant hyper-parameter  $\beta$  is the temperature to control simplex values, and we report the corresponding results under different  $\beta$  values in Figure 6. Increasing the  $\beta$  value from 0.001 to 0.005 encourages the loss value to assign more cost weights to the worst groups, consistently improving *F1-score* and *G-mean*. Additionally, *Specificity* achieves the highest value at  $\beta = 0.01$ , close to the case when  $\beta = 0.005$ .

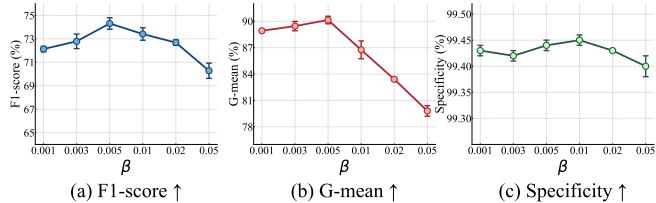


Figure 6. The comprehensive performance of GDR-CIL with error bars by varying  $\beta$  values on CIC-IDS2017 dataset (5 runs).

## 6. Conclusions and Limitations

**Empirical Findings.** This work proposes a simple yet effective cost-sensitive approach **GDR-CIL** for imbalanced network traffic classification. The use of group distributionally robust optimization suppresses the class imbalance effect, and we translate the optimization steps into a Stackelberg game. Extensive results reveal the potential of our approach in risk-sensitive and class-imbalanced scenarios.

**Limitations and Future Extensions.** Though our approach exhibits overall performance superiority with a clear interpretation, some additional configurations are still required in setups. Here, we leave a more optimal grouping mechanism design as promising explorations in the future.

## Acknowledgements

This work is funded by the National Natural Science Foundation of China (NSFC) with the Number # 62306326.

## References

Bårli, E. M., Yazidi, A., Viedma, E. H., and Haugerud, H. Dos and ddos mitigation using variational autoencoders. *Computer Networks*, 199:108399, 2021.

Breton, M., Alj, A., and Haurie, A. Sequential stackelberg equilibria in two-person games. *Journal of Optimization Theory and Applications*, 59:71–97, 1988.

Cao, K., Wei, C., Gaidon, A., Arechiga, N., and Ma, T. Learning imbalanced datasets with label-distribution-aware margin loss. *Advances in neural information processing systems*, 32, 2019.

Chawla, N. V., Bowyer, K. W., Hall, L. O., and Kegelmeyer, W. P. Smote: synthetic minority over-sampling technique. *Journal of artificial intelligence research*, 16:321–357, 2002.

Chou, H.-P., Chang, S.-C., Pan, J.-Y., Wei, W., and Juan, D.-C. Remix: rebalanced mixup. In *Computer Vision–ECCV 2020 Workshops: Glasgow, UK, August 23–28, 2020, Proceedings, Part VI 16*, pp. 95–110. Springer, 2020.

Cui, Y., Jia, M., Lin, T.-Y., Song, Y., and Belongie, S. Class-balanced loss based on effective number of samples. In *Proceedings of the IEEE/CVF conference on computer vision and pattern recognition*, pp. 9268–9277, 2019.

Das, S., Mullick, S. S., and Zelinka, I. On supervised class-imbalanced learning: An updated perspective and some key challenges. *IEEE Transactions on Artificial Intelligence*, 3(6):973–993, 2022.

Ding, H., Chen, L., Dong, L., Fu, Z., and Cui, X. Imbalanced data classification: A knn and generative adversarial networks-based hybrid approach for intrusion detection. *Future Generation Computer Systems*, 131:240–254, 2022.

Dong, S. Multi class svm algorithm with active learning for network traffic classification. *Expert Systems with Applications*, 176:114885, 2021.

Douzas, G. and Bacao, F. Effective data generation for imbalanced learning using conditional generative adversarial networks. *Expert Systems with applications*, 91:464–471, 2018.

D’Angelo, G. and Palmieri, F. Network traffic classification using deep convolutional recurrent autoencoder neural networks for spatial–temporal features extraction. *Journal of Network and Computer Applications*, 173:102890, 2021.

Elreedy, D. and Atiya, A. F. A comprehensive analysis of synthetic minority oversampling technique (smote) for handling class imbalance. *Information Sciences*, 505:32–64, 2019.

Fernando, K. R. M. and Tsokos, C. P. Dynamically weighted balanced loss: class imbalanced learning and confidence calibration of deep neural networks. *IEEE Transactions on Neural Networks and Learning Systems*, 33(7):2940–2951, 2021.

Goodfellow, I., Pouget-Abadie, J., Mirza, M., Xu, B., Warde-Farley, D., Ozair, S., Courville, A., and Bengio, Y. Generative adversarial nets. *Advances in neural information processing systems*, 27, 2014.

Guo, Y., Xiong, G., Li, Z., Shi, J., Cui, M., and Gou, G. Combating imbalance in network traffic classification using gan based oversampling. In *2021 IFIP Networking Conference (IFIP Networking)*, pp. 1–9. IEEE, 2021.

Gupta, N., Jindal, V., and Bedi, P. Cse-ids: Using cost-sensitive deep learning and ensemble algorithms to handle class imbalance in network-based intrusion detection systems. *Computers & Security*, 112:102499, 2022.

Huang, Z. A., Sang, Y., Sun, Y., and Lv, J. Neural network with absent minority class samples and boundary shifting for imbalanced data classification. *Neural Computing and Applications*, 35(12):8937–8953, 2023.

Khan, S. H., Hayat, M., Bennamoun, M., Sohel, F. A., and Togneri, R. Cost-sensitive learning of deep feature representations from imbalanced data. *IEEE transactions on neural networks and learning systems*, 29(8):3573–3587, 2017.

Khanam, S., Ahmedy, I., Idris, M. Y. I., and Jaward, M. H. Towards an effective intrusion detection model using focal loss variational autoencoder for internet of things (iot). *Sensors*, 22(15):5822, 2022.

Li, T. and Sethi, S. P. A review of dynamic stackelberg game models. *Discrete & Continuous Dynamical Systems-B*, 22(1):125, 2017.

Lin, T.-Y., Goyal, P., Girshick, R., He, K., and Dollár, P. Focal loss for dense object detection. In *Proceedings of the IEEE international conference on computer vision*, pp. 2980–2988, 2017.

Lin, Y.-D., Liu, Z.-Q., Hwang, R.-H., Nguyen, V.-L., Lin, P.-C., and Lai, Y.-C. Machine learning with variational autoencoder for imbalanced datasets in intrusion detection. *IEEE Access*, 10:15247–15260, 2022.

Liu, X.-Y., Wu, J., and Zhou, Z.-H. Exploratory undersampling for class-imbalance learning. *IEEE Transactions on Systems, Man, and Cybernetics, Part B (Cybernetics)*, 39(2):539–550, 2008.

Lloyd, S. Least squares quantization in pcm. *IEEE transactions on information theory*, 28(2):129–137, 1982.

Lotfollahi, M., Jafari Siavoshani, M., Shirali Hosseini Zade, R., and Saberian, M. Deep packet: A novel approach for encrypted traffic classification using deep learning. *Soft Computing*, 24(3):1999–2012, 2020.

Madabushi, H. T., Kochkina, E., and Castelle, M. Cost-sensitive bert for generalisable sentence classification on imbalanced data. In *Proceedings of the Second Workshop on Natural Language Processing for Internet Freedom: Censorship, Disinformation, and Propaganda*, pp. 125–134, 2019.

Monshizadeh, M., Khatri, V., Gamdou, M., Kantola, R., and Yan, Z. Improving data generalization with variational autoencoders for network traffic anomaly detection. *IEEE Access*, 9:56893–56907, 2021.

Moustafa, N. and Slay, J. Unsw-nb15: a comprehensive data set for network intrusion detection systems (unsw-nb15 network data set). In *2015 military communications and information systems conference (MilCIS)*, pp. 1–6. IEEE, 2015.

Nguyen, T. T. and Armitage, G. A survey of techniques for internet traffic classification using machine learning. *IEEE communications surveys & tutorials*, 10(4):56–76, 2008.

Park, S. and Park, H. Combined oversampling and undersampling method based on slow-start algorithm for imbalanced network traffic. *Computing*, 103(3):401–424, 2021.

Rahimian, H. and Mehrotra, S. Frameworks and results in distributionally robust optimization. *Open Journal of Mathematical Optimization*, 3:1–85, 2022.

Rose, K., Eldridge, S., and Chapin, L. The internet of things: An overview. *The internet society (ISOC)*, 80:1–50, 2015.

Sagawa, S., Koh, P. W., Hashimoto, T. B., and Liang, P. Distributionally robust neural networks. In *International Conference on Learning Representations*, 2019.

Sampath, V., Maurtua, I., Aguilar Martin, J. J., and Gutierrez, A. A survey on generative adversarial networks for imbalance problems in computer vision tasks. *Journal of big Data*, 8:1–59, 2021.

Sharafaldin, I., Lashkari, A. H., Ghorbani, A. A., et al. Toward generating a new intrusion detection dataset and intrusion traffic characterization. *ICISSP*, 1:108–116, 2018.

Shelke, M. S., Deshmukh, P. R., and Shandilya, V. K. A review on imbalanced data handling using undersampling and oversampling technique. *Int. J. Recent Trends Eng. Res.*, 3(4):444–449, 2017.

Tavallaei, M., Bagheri, E., Lu, W., and Ghorbani, A. A. A detailed analysis of the kdd cup 99 data set. In *2009 IEEE symposium on computational intelligence for security and defense applications*, pp. 1–6. Ieee, 2009.

Telikani, A. and Gandomi, A. H. Cost-sensitive stacked auto-encoders for intrusion detection in the internet of things. *Internet of Things*, 14:100122, 2021.

Telikani, A., Gandomi, A. H., Choo, K.-K. R., and Shen, J. A cost-sensitive deep learning-based approach for network traffic classification. *IEEE Transactions on Network and Service Management*, 19(1):661–670, 2021.

Wang, J., Yan, X., Liu, L., Li, L., and Yu, Y. Cttgan: Traffic data synthesizing scheme based on conditional gan. *Sensors*, 22(14):5243, 2022.

Wang, P., Li, S., Ye, F., Wang, Z., and Zhang, M. Packetgan: Exploratory study of class imbalance for encrypted traffic classification using cgan. In *ICC 2020-2020 IEEE International Conference on Communications (ICC)*, pp. 1–7. IEEE, 2020.

Wang, Q., Luo, Z., Huang, J., Feng, Y., Liu, Z., et al. A novel ensemble method for imbalanced data learning: bagging of extrapolation-smote svm. *Computational intelligence and neuroscience*, 2017, 2017.

Wang, Q., Feng, Y., Huang, J., Lv, Y., Xie, Z., and Gao, X. Large-scale generative simulation artificial intelligence: The next hotspot. *The Innovation*, 4(6), 2023.

Wang, S., Liu, W., Wu, J., Cao, L., Meng, Q., and Kennedy, P. J. Training deep neural networks on imbalanced data sets. In *2016 international joint conference on neural networks (IJCNN)*, pp. 4368–4374. IEEE, 2016.

Xie, Y., Qiu, M., Zhang, H., Peng, L., and Chen, Z. Gaussian distribution based oversampling for imbalanced data classification. *IEEE Transactions on Knowledge and Data Engineering*, 34(2):667–679, 2020.

Xu, X., Li, J., Yang, Y., and Shen, F. Toward effective intrusion detection using log-cosh conditional variational autoencoder. *IEEE Internet of Things Journal*, 8(8):6187–6196, 2020.

Yan, B., Han, G., Huang, Y., and WANG, X. New traffic classification method for imbalanced network data. *Journal of Computer Applications*, 38(1):20, 2018.

Zavrak, S. and Iskefiyeli, M. Anomaly-based intrusion detection from network flow features using variational autoencoder. *IEEE Access*, 8:108346–108358, 2020.

Zhang, H., Cisse, M., Dauphin, Y. N., and Lopez-Paz, D. mixup: Beyond empirical risk minimization. *arXiv preprint arXiv:1710.09412*, 2017.

Zhang, H., Huang, L., Wu, C. Q., and Li, Z. An effective convolutional neural network based on smote and gaussian mixture model for intrusion detection in imbalanced dataset. *Computer Networks*, 177:107315, 2020.

Zhao, Y., Hao, K., Tang, X.-s., Chen, L., and Wei, B. A conditional variational autoencoder based self-transferred algorithm for imbalanced classification. *Knowledge-Based Systems*, 218:106756, 2021.

Zhu, D., Ying, Y., and Yang, T. Label distributionally robust losses for multi-class classification: Consistency, robustness and adaptivity. In *International Conference on Machine Learning*, pp. 43289–43325. PMLR, 2023a.

Zhu, S., Xu, X., Gao, H., and Xiao, F. Cmtsnn: A deep learning model for multi-classification of abnormal and encrypted traffic of internet of things. *IEEE Internet of Things Journal*, 2023b.

Zuech, R., Hancock, J., and Khoshgoftaar, T. M. Detecting web attacks using random undersampling and ensemble learners. *Journal of Big Data*, 8(1):75, 2021.

## A. Benchmark Details

CIC-IDS2017 (Sharafaldin et al., 2018) is a commonly used intrusion detection dataset with 15 network traffic classes, including “BENIGN”, which refers to normal, harmless network traffic, and 14 kinds of the most up-to-date common attacks. It provides CSV (Comma-Separated Values) files for machine and deep learning purposes, each containing 78 different features, such as flow duration, maximum packet length, minimum packet length, number of forward packets, etc.

NSL-KDD (Tavallaei et al., 2009) stands for “NSL-KDD Data set for network-based Intrusion Detection Systems”. It consists of four sub-datasets provided in CSV format: KDDTest+, KDDTest-21, KDDTrain+, KDDTrain+\_20Percent, where KDDTest-21 and KDDTrain+\_20Percent are subsets of KDDTrain+ and KDDTest+, respectively. There are “Normal” and 4 kinds of different types of attacks in these sets, including “Denial of Service (DoS)”, “Probe”, “User-to-Root (U2R)”, and “Remote to Local (R2L)”, as depicted in Figure 2b. Each record in the dataset contains 41 features.

UNSW-NB15 dataset (Moustafa & Slay, 2015) is an intrusion evaluation dataset published by the University of New South Wales in 2015, with 10 network traffic classes consisting of “Normal” and 9 types of attacks. It includes a training set (UNSW\_NB15\_training-set) and a testing set (UNSW\_NB15\_testing-set), both in CSV format, each set including 42 features.

## B. Baseline Details

Here, we detail the mentioned baselines in this work as follows:

1. Expected Risk Minimization (ERM) loss: it assigns the same weight to all classes and adopts the standard cross entropy as the loss function in optimization.
2. Focal loss (Lin et al., 2017): it adds a factor  $(1 - p_t)^\gamma$  to the standard cross-entropy criterion to down-weight the loss assigned to well-classified samples.
3. Class-Balanced (CB) (Cui et al., 2019): it utilizes the effective number of samples, calculated by  $(1 - \beta^{n_i}) / (1 - \beta)$ , for each class to re-balance the loss.
4. Mixup with Deferred Re-Weighting (Mixup-DRW) (Zhang et al., 2017): it constructs virtual examples as the linear interpolation of features of two random samples from the training set and their labels, by using a mixing factor sampled from the beta distribution.
5. Remix with Deferred Re-Weighting (Remix-DRW) (Chou et al., 2020): it mixes features of two samples in Mixup fashion and assigns the label that prefers to the minority class by providing a disproportionately higher weight to the minority class.
6. Label-Distribution-Aware Margin loss with Deferred Re-Weighting (LDAM-DRW) (Cao et al., 2019): it enforces a class-dependent margin, depending on the label distribution, for multiple classes of the form  $\gamma_j = \frac{C}{n_j^{1/4}}$ .
7. Label Distributionally Robust loss with Kullback-Leibler divergence (LDR-KL) (Zhu et al., 2023a): with each class label assigned a distributional weight, it formulates the loss in the worst case of the distributional weights regularized by KL divergence function.

## C. Implementation Details

**Training-Validation-Testing Dataset Split.** We describe the dataset-splitting strategy for all benchmarks. For CIC-IDS2017 dataset, as shown in Figure (2a), the quantities of majority classes are highly greater than minority ones, thus we adopt an extraction strategy as the same in (Wang et al., 2022). We randomly extract 10,000 traffic samples from the classes with data quantities exceeding 10,000 while keeping the quantities of other classes unchanged. Then we randomly split the dataset into training (56%), validation (14%), and testing (30%) sets. The training set consists of 91,784 samples, the validation set 22,946 samples, and the testing set the remaining 49,171 samples.

For NSL-KDD dataset, we merge KDDTest-21 and KDDTrain+\_20Percent sets, introduced in Appendix A, into one set. Then we perform the same training-validation-testing set split operation as CIC-IDS2017 dataset. The training set consists of 20,743 samples, the validation set 5,186 samples, and the testing set the remaining 11,113 samples.

For UNSW-NB15 dataset, we combine the training and testing sets, introduced in Appendix A, into one set. Considering the high imbalance among classes as shown in Figure (2c), we adopt the same extraction strategy as for CIC-IDS2017 dataset. Then we use the same process of splitting the dataset into training, validation, and testing sets as CIC-IDS2017 dataset. The training set consists of 37,346 samples, the validation set 9,337 samples, and the testing set the remaining 20,008 samples.

The training set is to train the MLP, the validation set is to tune hyper-parameters, such as the learning rate, and to determine when to stop training, and the testing set serves as an independent evaluation set to assess the generalization performance of the trained MLP. Note that the testing set is not used for any training-related tasks to ensure unbiased evaluation.

**Training Details.** Note that the number of groups  $K$  is heuristically defined, and the class clustering results are based on the classification performance in the initial standard training and the number of training samples in each class. We treat the regularizer associated  $B$  and the temperature  $\beta$  as hyper-parameters. For CIC-IDS2017 dataset, we set  $K = 8$ ,  $B = 0.25$ , and  $\beta = 0.005$  based on the F1-score performance on the validation dataset. In the same way, we set  $K = 5$ ,  $B = 0.02$ ,  $\beta = 0.15$  in NSL-KDD dataset, and  $K = 10$ ,  $B = 0.02$ ,  $\beta = 0.1$  in UNSW-NB15 dataset given the validation dataset performance.

We provide the grouping results for each dataset. In CIC-IDS2017 dataset, the fifteen classes are divided into 8 groups. The first group contains “BENIGN”. The second group includes “DDoS”, “DoS GoldenEye”, “DoS Hulk”, and “PortScan”. The third group comprises “SSH-Patator”, “DoS Slowhttptest”, “DoS slowloris”, and “FTP-Patator”. The fourth group combines “Bot” and “Web Attack Brute Force”. The remaining four classes represent four more groups. The NSL-KDD dataset has 5 groups, each representing a class. Similarly, UNSW-NB15 dataset has 10 groups.

To avoid overfitting, the MLP is augmented by the dropout module with a learning rate of 0.2. The parameters in the MLP neural network are initialized by a truncated normal distribution with a standard deviation of  $3e - 2$ . The batch size is set to be 128 as default. In the training stage, we set up a learning rate scheduler that dynamically adjusts the learning rate based on the validation loss. Concretely, if the validation loss does not improve for six epochs, the learning rate will be reduced by half. The scheduler will not reduce the learning rate below  $1e - 6$ . We implemented early stopping to halt training if validation loss stagnates for 30 consecutive epochs. The network is trained for a maximum of 200 epochs.

**Python Implementation.** This work’s implementation is largely inspired by the group distributionally robust optimization method in (Sagawa et al., 2019), where the GitHub link is ([https://github.com/kohpangwei/group\\_DRO](https://github.com/kohpangwei/group_DRO)). Further, we attach the loss function of **GDR-CIL** methods in Python as follows.

```

1 import numpy as np
2 import torch
3
4 class LossComputer:
5     def __init__(self,
6                  criterion=nn.CrossEntropyLoss(reduction='none'),
7                  n_groups: int,
8                  group_counts: torch.Tensor,
9                  B: float = 0.25,
10                 beta: float = 0.005,
11                 normalize_loss: bool=False,
12                 device: torch.device,
13                 ):
14         self.criterion = criterion
15         self.device = device
16         self.beta = beta
17         self.normalize_loss = normalize_loss
18         self.B = torch.tensor(B).to(device)
19         self.n_groups = n_groups
20         self.group_counts = group_counts.to(device)
21         self.group_frac = self.group_counts / self.group_counts.sum()
22         self.adv_probs = torch.ones(self.n_groups).cuda() / self.n_groups
23
24     def loss(self, yhat, y, g=None):
25         per_sample_losses = self.criterion(yhat, y)
26         group_loss, group_count = self.compute_group_avg(per_sample_losses, g)
27         actual_loss, weights = self.compute_robust_loss(group_loss, group_count)
28         return actual_loss
29

```

```

30
31     def compute_group_avg(self, losses, group_idx):
32         group_map = (group_idx == torch.arange(self.n_groups).unsqueeze(1).long().cuda()).float()
33         group_count = group_map.sum(1)
34         group_denom = group_count + (group_count == 0).float()
35         group_loss = (group_map @ losses.view(-1)) / group_denom
36         return group_loss, group_count
37
38     def compute_robust_loss(self, group_loss, group_count):
39         adjusted_loss = group_loss
40         if torch.all(self.adj > 0.0):
41             adjusted_loss += self.adj / torch.sqrt(self.group_counts)
42         if self.normalize_loss:
43             adjusted_loss = adjusted_loss / (adjusted_loss.sum())
44         self.adv_probs = self.adv_probs * torch.exp(self.step_size * adjusted_loss.data)
45         self.adv_probs = self.adv_probs / (self.adv_probs.sum())
46         robust_loss = group_loss @ self.adv_probs
47         return robust_loss, self.adv_probs

```

Listing 1. Loss function in **GDR-CIL**

## D. Platform and Computational Tools

Throughout the paper, we use the Pytorch as the default toolkit to conduct all experiments.